

Mixture of Experts for Node Classification

Yu Shi*, Yiqi Wang*[†], WeiXuan Lang, Jiaxin Zhang, Pan Dong[†], Aiping Li[†]

College of Computer Science and Technology
National University of Defense Technology
Changsha 410073

Abstract

Nodes in the real-world graphs exhibit diverse patterns in numerous aspects, such as degree and homophily. However, most existent node predictors fail to capture a wide range of node patterns or to make predictions based on distinct node patterns, resulting in unsatisfactory classification performance. In this paper, we reveal that different node predictors are good at handling nodes with specific patterns and only apply one node predictor uniformly could lead to suboptimal result. To mitigate this gap, we propose a mixture of experts framework, MOE-NP, for node classification. Specifically, MOE-NP combines a mixture of node predictors and strategically selects models based on node patterns. Experimental results from a range of real-world datasets demonstrate significant performance improvements from MOE-NP.

Introduction

Node classification, which aims to predict the class of nodes in a graph, has a wide range of applications (Tang, Aggarwal, and Liu 2016; Xiao et al. 2022), such as citation networks and co-author networks (Lin et al. 2020; Xiao et al. 2022). The key to node classification tasks lies in node representation learning (Jin et al. 2021), which has been theoretically and empirically proven to be one of the key strengths of Graph Neural Networks (GNNs) (Hamilton, Ying, and Leskovec 2017). GNNs typically refine node representations through information aggregation and feature transformation among the nodes, and have achieved impressive performance in various graph-related tasks, such as social analysis (Ben Yahia 2024), recommendation system (Wu et al. 2022) and traffic prediction (Yu, Yin, and Zhu 2018).

Most existent GNN models are designed based on the homophily assumption (Bi et al. 2024; Zheng, Luan, and Chen 2024; Platonov et al. 2024), i.e., nodes tend to be similar with those connected to them. However, this assumption is not always true. There exist numerous heterophilic graphs in reality, such as the social network in a dating website (Wang et al. 2024), where numerous users tend to follow people of different genders. To solve node classification in these scenarios, several studies propose to integrate information from broader neighborhoods so as to strengthen the relationships

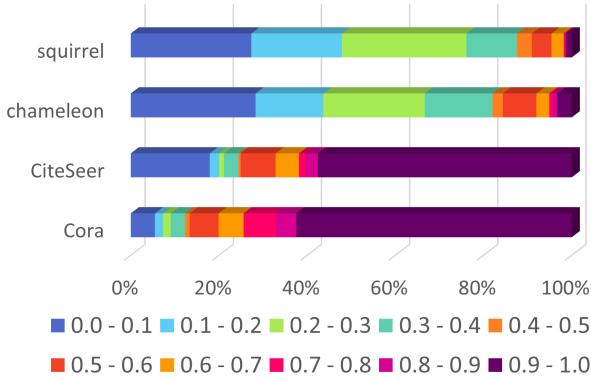
between originally-unconnected nodes. For instance, MixHop (Abu-El-Haija et al. 2019) repeatedly mixes feature representations of neighbors at various distances. GeomGCN (Pei et al. 2020) proposes to add virtual nodes in feature aggregation. WRGCN (Suresh et al. 2021) constructs a modified computation graph to enhance the connections and information for disassortative nodes. Furthermore, some recent work (Luan et al. 2022; Chen et al. 2023) proposes to deal with this heterophily challenge in a node-wise manner, given the consideration that different nodes in the same graph can be faced with distinct heterophily challenges.

While heterophily issue has been widely studied, some latest research (Ma et al. 2021; Mao et al. 2024) suggests that node classification is essentially related to the node pattern, rather than merely the label homophily. However, the node pattern is quite complex, which can be described from various perspectives, including label homophily, structure information and attribute information. In addition, nodes within the same graph can possess diverse node patterns from different perspectives. This naturally raises a problem: *Do nodes with different node patterns within the same graph require distinct node predictors?*

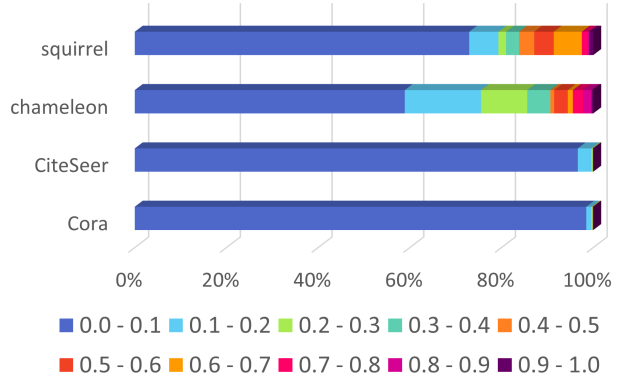
To answer this question, we first have conducted some empirical investigations over node patterns. We have observed that nodes with different patterns in one graph require distinct node classifiers and their preferences for classifiers are affected by numerous factors. Furthermore, we have noticed that the classifier preference is not only related to node pattern, but also associated with the overall graph context, as suggested in previous study (Mao et al. 2024). Based on these observation, we then propose MOE-NP, a mixture-of-expert model for the node classification task, which consists of a bunch of diverse node predictors and a specially designed gating network. The gating network is able to adaptively assign experts to each node according to both its local node pattern and the overall graph context. Extensive experiments have shown the superior performance of the proposed MOE-NP. Specifically, it surpasses the best baseline on PubMed and Actor datasets by 4.4% and 3.4% in accuracy. In addition, a theoretical analysis is provided to demonstrate the rationality of MOE-NP.

*Equal contribution.

[†]Corresponding authors.



(a) homophily diversity



(b) degree diversity

Figure 1: The distribution of node homophily and degree across different datasets

Preliminary

In this section, We investigate node patterns within the same graph from different perspectives and their influence towards the classifiers. Some notations and backgrounds are first introduced, and then we discuss the empirical observations and key insights.

Notations and Backgrounds

We denote an undirected graph without self-loops as $\mathcal{G} = (\mathcal{V}, \mathcal{E})$, where $\mathcal{V} = \{v_i\}_{i=1}^n$ is the node set and $\mathcal{E} \subseteq \mathcal{V} \times \mathcal{V}$ is the edge set. Let $\mathcal{N}(v_i)$ denote the neighbors of node v_i . $\mathbf{A} \in \mathbb{R}^{n \times n}$ denotes the adjacency matrix, and \mathbf{D} represents the diagonal matrix standing for the degree matrix such that $\mathbf{D}_{ii} = \sum_{j=1}^n \mathbf{A}_{ij}$. Let $\tilde{\mathbf{A}}$ and $\tilde{\mathbf{D}}$ be the corresponding matrices with self-loops, i.e., $\tilde{\mathbf{A}} = \mathbf{A} + \mathbf{I}$ and $\tilde{\mathbf{D}} = \mathbf{D} + \mathbf{I}$, where \mathbf{I} is the identity matrix. $\mathbf{X} \in \mathbb{R}^{n \times d}$ denotes the initial node feature matrix, where d is the number of dimensions. We use y to denote the ground-truth node label and y_i denote the label of node i . In this paper, we define homophily h on graph \mathcal{G} as

$$h(\mathcal{G}) = \frac{1}{|\mathcal{V}|} \sum_{v_i \in \mathcal{V}} \frac{|\{u \mid u \in \mathcal{N}(v_i), y_u = y_{v_i}\}|}{\mathbf{D}_{ii}}. \quad (1)$$

where $h(\mathcal{G})$ is the average node homophily value for Graph \mathcal{G} , within the range of $[0, 1]$.

Most Graph Neural Networks (GNNs) are designed to use low-pass filters to refine node representation, which tend to smooth node features across the graph based on the homophily assumption. On the contrary, the high-pass GNNs are designed to capture differences between a node and its neighbors, which are more suitable for heterophilic graphs, where nodes tend to connect with different counterparts. In addition, there exist some models, such as multilayer perceptrons (MLPs), not aggregating neighbor information. Instead, they solely transform features based on the its own data, ignoring the graph structure.

Empirical Study

As shown in Figure 1, nodes in the same graph can vary in patterns from different perspectives, such as homophily and degree. Regardless of whether the overall graph is homophilic or heterophilic, the node distributions in terms of homophily and degree values can exhibit significant differences within one graph. Specifically, there can exist considerable heterogeneous nodes in a homophilic graph, and vice versa.

To explore the effect of node patterns towards node classification, a series of preliminary study have been conducted. Specifically, we divide nodes from one dataset into five groups based on its homophily values, and examine their preferences for different node classifiers. The results of both a homophilic graph and a heterotrophic graph are demonstrated in Figure 2. It is obvious that nodes from different homophily group hold diverse preferences for node classifiers. Also, this preference difference is not related to the homophily group, but the overall graph homophily, given the observation that best classifiers for nodes from low and medium groups are not the same between Chameleon and PubMed. To reveal the diversity of node patterns and its influence for node classification, we further divide one homophily group into five separate sets based on the node degree value. As shown in Figure 2c, even within the same homophily group, the degree of nodes influences the effectiveness of different node predictors.

The varying effectiveness of classifiers across different homophily and degree groups suggests that the complex node patterns play significant role in node classification, and the node patterns are supposed to be illustrated from diverse perspectives. In addition, both local properties and the broader context of the graph affect the preference for node classifiers. These observations highlight the necessity of assigning different classifiers to different nodes based on both their node patterns from various aspects and the overall graph context.

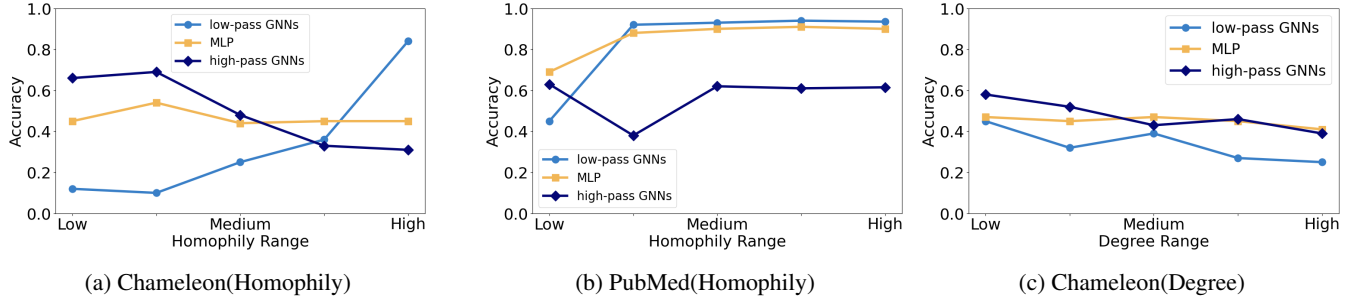


Figure 2: Figure(a) and (b) show the classifier preferences for nodes from different homophily groups in Chameleon and PubMed, where Chameleon is a typical heterophilic graph and PubMed is a homophilic one. Figure(c) further demonstrates the classification performance of different node classifiers in node groups with various degree values from the low homophily group in Figure(a).

Theoretical analysis

This section provides a theoretical analysis to support the necessity for different node predictors for nodes with diverse node patterns. We use the Contextual Stochastic Block Model (CSBM) (Baranwal, Fountoulakis, and Jagannath 2021), a generative model commonly employed to produce graph structures and node features. Typically, CSBMs assume graphs following a uniform pattern. It generates edges following nodes with the same label connected with probability p , while nodes with different labels are connected with probability q . We have a Contextual Stochastic Block Model (CSBM) as

$$(\mathbf{A}, \mathbf{X}) \sim \text{CSBM}(n, p, q, \boldsymbol{\mu}, \boldsymbol{\nu}), \quad (2)$$

where n represents the total number of nodes, and $\boldsymbol{\mu}$ and $\boldsymbol{\nu}$ denote the average feature vectors for different node classes with $\|\boldsymbol{\mu}\|, \|\boldsymbol{\nu}\| \leq 1$. Feature vectors drawn from a Gaussian distribution $\mathcal{N}(\boldsymbol{\mu}, \sigma^2 \mathbf{I})$, where $\sigma^2 \mathbf{I}$ is the covariance matrix, with \mathbf{I} representing the identity matrix. Without loss of generality, we assume that $p - q \leq 0$. Similarly, we define another CSBM as

$$(\mathbf{A}', \mathbf{X}') \sim \text{CSBM}(n', p', q', \boldsymbol{\mu}, \boldsymbol{\nu}). \quad (3)$$

We use a linear classifier with parameters $\mathbf{w} \in \mathbb{R}^d$ and $b \in \mathbb{R}$. The predicted labels can be represented by

$$\hat{y} = \sigma(\tilde{\mathbf{X}}\mathbf{w} + b\mathbf{1}), \quad (4)$$

where $\sigma(x) = (1 + e^{-x})^{-1}$ denotes the sigmoid function. We utilize Simplified Graph Convolutional networks (SGC) characterized by low-pass filters, which are defined as

$$\tilde{\mathbf{X}} = \mathbf{D}^{-1} \mathbf{A} \mathbf{X}. \quad (5)$$

We use the binary cross-entropy loss as

$$L(\mathcal{V}, \mathbf{w}, b) = -\frac{1}{|\mathcal{V}|} \sum_{i \in \mathcal{V}} y_i \log(\hat{y}_i) + (1 - y_i) \log(1 - \hat{y}_i), \quad (6)$$

where \mathcal{V} are test samples.

(Baranwal, Fountoulakis, and Jagannath 2021) shows that the optimal linear classifier is given by $\mathbf{w}^* = R \frac{\boldsymbol{\nu} - \boldsymbol{\mu}}{\|\boldsymbol{\nu} - \boldsymbol{\mu}\|}$ and $b^* = -\frac{1}{2} \langle \boldsymbol{\nu} + \boldsymbol{\mu}, \mathbf{w}^* \rangle$. It is assumed that the distance between $\boldsymbol{\mu}$ and $\boldsymbol{\nu}$ is large, satisfying $\|\boldsymbol{\nu} - \boldsymbol{\mu}\| = \Omega\left(\frac{\log n}{dn(p+q)}\right)$.

Following Assumptions 1 and 2 in (Baranwal, Fountoulakis, and Jagannath 2021), the graph size n must be sufficiently large, with $\omega(d \log d) \leq n \leq O(\text{poly}(d))$, and not too sparse, ensuring $p, q, p', q' = \omega\left(\frac{\log^2(n)}{n}\right)$.

The following explores the optimal classifier with parameters \mathbf{w}^*, b^* as it performs on various general patterns $(\mathbf{A}', \mathbf{X}')$. We aim to demonstrate that a single classifier cannot effectively fit all node patterns.

Theorem 1. *If $(p - q)(p' - q') \leq 0$, the following inequality*

$$L(\mathbf{A}', \mathbf{X}', \mathbf{w}^*, b^*) \geq \frac{R(q' - p')}{2(p' + q')} \|\boldsymbol{\mu} - \boldsymbol{\nu}\| (1 + o(1)), \quad (7)$$

holds with $\mathbf{w}^*, b^* = \arg \min_{\mathbf{w}, b} L(\mathbf{A}, \mathbf{X}, \mathbf{w}, b)$.

Theorem 2. *If $(p - q)(p' - q') \geq 0$ and $\|\boldsymbol{\nu} - \boldsymbol{\mu}\| = \Omega\left(\frac{\log n}{dn(p'+q')}\right)$, we have*

$$L(\mathbf{A}', \mathbf{X}', \mathbf{w}^*, b^*) \leq C \exp\left(-\frac{R(p' - q')}{2(p' + q')} \|\boldsymbol{\mu} - \boldsymbol{\nu}\| (1 - o(1))\right). \quad (8)$$

Remark. Theorem 1 suggests that the generalization error becomes significant when a single classifier attempts to generalize across distributions beyond the homophily shift. Similarly, Theorem 2 indicates that variations in degree can disrupt the linear separability condition, resulting in the absence of a linearly separable hyperplane. A single classifier demonstrates satisfactory generalization performance under distributional shifts only in limited cases, and even then, this improvement becomes apparent only as the sample size increases. All detailed proofs are provided in Appendix .

Method

Based on the preliminary study, nodes within the same graph can exhibit diverse node patterns from different perspectives, and this affects their preference for node predictors significantly. To accommodate the node pattern diversity, this paper proposes a Mixture of Experts (MoE) framework to solve node classification, which is able to assign node predictors with different weights to each node based on its node patterns. There are several challenges to be addressed. First, how to accurately define node patterns given they are complex and multi-modal? Second, how to appropriately com-

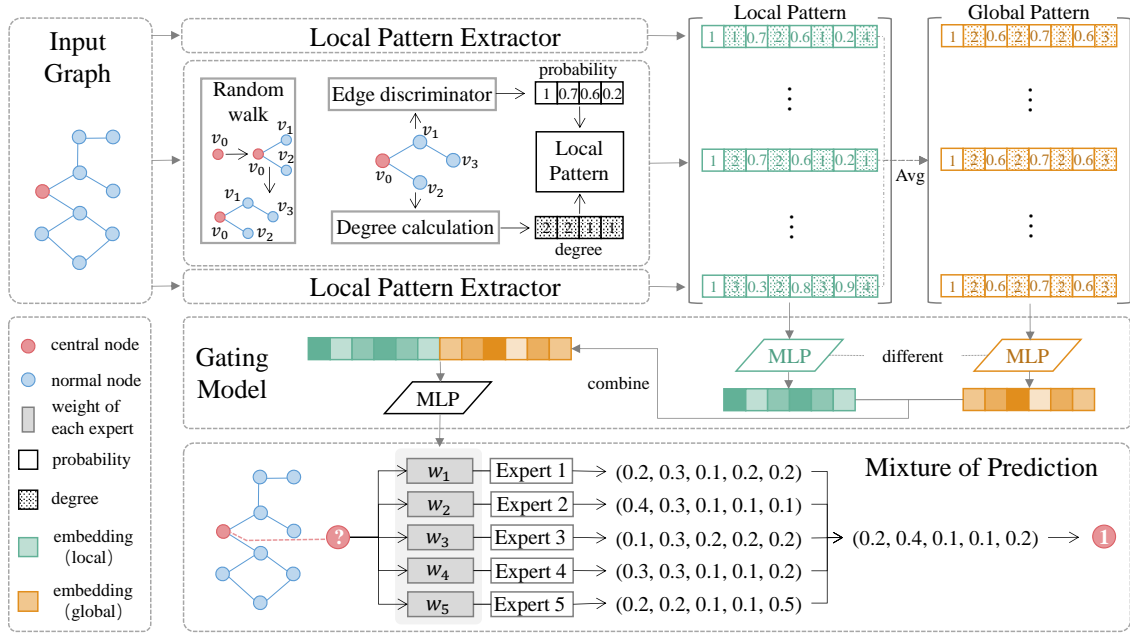


Figure 3: The overall framework of the proposed MOE-NP . For each node, the gating model will assign different weights for each expert based on the node’s pattern.

bine different node predictors for distinct node? In the following sections, we will give an overall framework description, and then illustrate how we address these challenges.

MOE-NP – A General Framework

The overall MOE-NP framework is illustrated in Figure 3, which consists of two main components, the node pattern extractor and the gating model. Specifically, the node pattern extractor is designed to extract multi-modal node patterns for each node. The gating model is developed to generate node-wise expert weights for different nodes based on their extracted node patterns. There are five common node predictors adopted as experts in the proposed MOE-NP , and more advanced experts can be easily added into the flexible MOE-NP framework.

Node Pattern Extractor

As revealed in the previous study, node patterns directly influence the classification performance of node predictors. Thus, it is essential to design a reasonable node pattern extractor for the proposed MOE-NP . However, this is not a trivial task. On the one hand, node patterns are naturally multi-modal and can vary in numerous aspects, such as the degree distribution and the label homophily distribution. On the other hand, label homophily distribution is hard to be accurately computed, given the absence of ground-truth labels in the test graph.

To solve these challenges, we carefully design a node pattern extractor component. To objectively reflect the local structure context for a given node, random walk sampling has been conducted for each node in its neighborhood. The sampled nodes are then formalize the local context for the

given node, where further pattern extraction is performed. In order to exploit the node pattern from the node feature modality and to overcome the absence of node label, MOE-NP proposes to learn an edge discriminator, an instance of multi-layer perceptron (MLP), to predict the pair relation between the target node and all the nodes, based on their node features in the local graph. To further enhance the structure information, we concatenate the degree information with its edge discriminator’s output in a node-wise manner, as demonstrated in Figure 3.

The Design of the Gating Model

Given the multi-modal local patterns provided by the node patten extractor, an appropriate gating model is desperate, which is supposed to dynamically assign weights to node classifiers for each node based on its patterns. As revealed in the previous study (Mao et al. 2024) and the preliminary analysis, the node classification is not only relevant to the local node patterns, but the overall graph pattern. For instance, nodes with relatively-low homophily values may require different node predictors, due to the variance of graph it belongs to. To reflect the overall graph context, MOE-NP proposes to generate a graph pattern via averaging all the local node patterns in a graph. Next, both the local pattern and the global pattern are transformed into the same embedding space by two learnable MLP models. The concatenated embedding from both the local and global perspectives are then serve as the input of the gating model. Finally, an MLP with the softmax function is applied to generate the final weight predictions, which is used to combine the prediction results from different experts in a node-wise manner.

models	Homophilic Datasets			Heterophilic Datasets				Avg Rank
	Cora	PubMed	Texas	Cornell	Wisconsin	Chameleon	Actor	
MLP	75.01 ± 2.29	87.78 ± 0.3	76.76 ± 4.55	78.11 ± 8.15	81.37 ± 6.63	49.25 ± 2.12	36.53 ± 0.78	6.14
GCN	87.26 ± 1.24	88.02 ± 0.49	62.43 ± 5.05	62.43 ± 3.3	60.59 ± 7.82	68.11 ± 1.32	30.57 ± 0.74	6.43
HighPass GCN	38.15 ± 2.21	63.74 ± 0.89	78.11 ± 4.43	59.73 ± 5.05	74.51 ± 5.11	59.50 ± 2.4	32.71 ± 1.11	6.71
ACMGCN	88.27 ± 1.15	89.74 ± 0.5	87.30 ± 2.97	77.57 ± 4.84	84.9 ± 2.78	68.62 ± 1.8	36.07 ± 1.29	3.29
LINK	78.91 ± 2.08	80.51 ± 0.7	65.41 ± 4.49	55.68 ± 7.07	61.57 ± 6.4	70.99 ± 2.16	24.26 ± 1.1	6.57
LSGNN	87.36 ± 0.89	89.33 ± 0.44	81.08 ± 3.63	79.73 ± 5.57	84.31 ± 4.02	74.12 ± 1.33	35.50 ± 1.29	3.57
GloGNN	88.31 ± 1.13	89.62 ± 0.35	84.32 ± 4.15	83.51 ± 4.26	87.06 ± 3.53	69.78 ± 2.42	37.35 ± 1.30	<u>2.43</u>
MOE-NP	89.31 ± 0.91	94.02 ± 0.33	86.76 ± 4.26	86.49 ± 5.54	85.29 ± 3.07	73.82 ± 2.1	40.74 ± 1.36	1.43

Table 1: The results of the node classification experiments on both homophilic and heterophilic datasets

Optimization Objective

The proposed MOE-NP aim at solving node classification tasks, thus a typical node classification loss is leveraged as the overall optimization objective as follows:

$$L_{MOE-NP} = \sum_{i=1}^n \log(1 + \exp(-y_i(\sum_{i=1}^t w_i E_i(x))))$$

where n denotes the total number of nodes in the training set, y_i represents the true label of node i , and the prediction result is derived from the outputs of multiple experts, weighted by w_j , which are determined by the gating model. The whole framework, including the edge discriminator and the gating model, is optimized in an end-to-end way under this objective. Detailed training process is discussed in Appendix .

Experiments

In this section, comprehensive experiments have been conducted to validate the effectiveness and rationality of the proposed MOE-NP . The experiments settings are first introduced, then the comparison of MOE-NP and the state-of-the-art baseline on different datasets are demonstrated. Next comes further analysis of the proposed MOE-NP .

Experimental settings.

Datasets. We have conducted experiments on seven widely-used datasets, including two homophilic datasets, Cora and Pubmed (Sen et al. 2008) and five heterophilic datasets, Texas, Wisconsin, Cornell, Chameleon, and Actor (Rozemberczki, Allen, and Sarkar 2021). For each dataset, 10 random splits are generated with 60% training, 20% validation, and 20 % testing partitions. In each split, the models are trained with 3 different random seeds, and the average performance and standard deviation are reported.

Baselines. Seven baselines have been adopted for comparison, including basic methods, such as MLP, common GCN (Kipf and Welling 2017)and high-pass GCN. Some latest methods that are specially designed for heterotrophic graphs have also been taken into consideration, such as ACMGCN (Luan et al. 2022), GloGNN (Li et al. 2022), LinkX (Lim et al. 2021) and LSGNN (Chen et al. 2023).

MOE-NP Implementations. In this work, we implement five commonly-used models as experts. They are GCN,

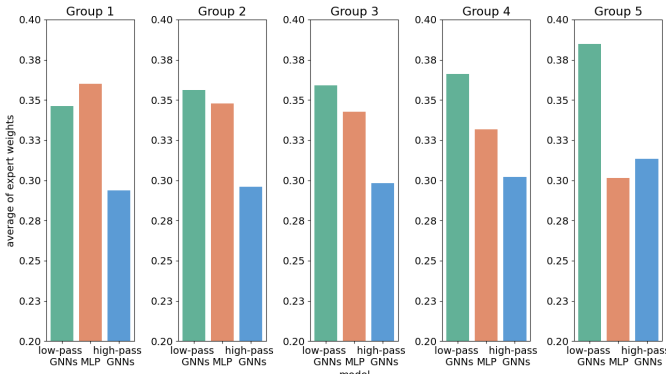
GCN with residual connect, High-pass GNN, High-pass GNN with residual connect, and MLP. Additional node predictors can be easily added as experts, given the flexibility of MOE-NP .

The Overall Performance Comparison

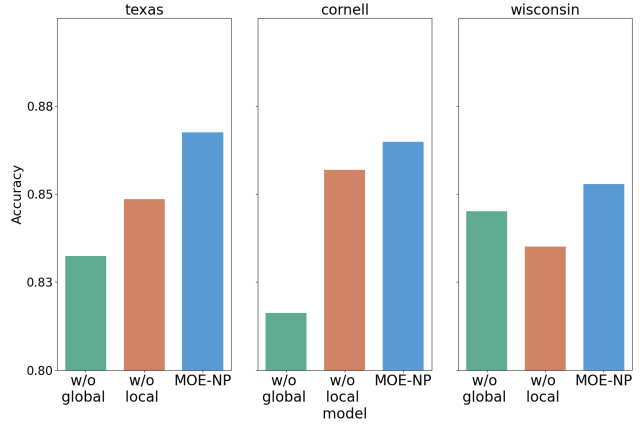
We have compared the proposed MOE-NP with seven baselines on seven datasets, including both the homophilic and heterophilic graphs. The results are shown in Table 1. The proposed MOE-NP has demonstrated impressive performance on both the homophilic and heterophilic graphs, achieving the best overall rank among all the methods. The basic baselines, such as MLP and GCN, tend to perform well only on specific groups, while MOE-NP leveraging several such baselines as experts can achieve significant improvements in terms of classification performance, even surpassing other SOTA baselines, such as ACMGNN and GloGNN. This demonstrates the effectiveness of the proposed MOE-NP .

Analysis of MOE-NP

In this section, we conduct some further analysis towards MOE-NP to demonstrate the rationality and effectiveness of its design. To examine the effectiveness of the gating model and the pattern extractor, we divide nodes in chameleon into five groups, following an increasing order of node homophily value, and then observe the expert weights assigned to different groups in MOE-NP . To simplify the analysis, we implement three basic models as experts. As shown in Figure 4a, the gating model generate different expert weights for node groups with different homophily characteristic, and the expert weight for the low-pass GNN is significantly higher in the node group with higher homophily values, which demonstrates the effectiveness of the weight allocation mechanism in MOE-NP . Also, we compare MOE-NP with an average weight allocation strategy as illustrated in Table 2 to further demonstrate the efficacy of the gating model. In addition, to validate the rationality of node extractor, we conduct an ablation study via excluding the global pattern part or the local pattern part. As shown in Figure 4b, either reducing the global pattern or the local pattern can cause a significant performance loss of MOE-NP , which shows the necessity of node patterns from both the local and global perspectives.



(a) The weights assigned to three experts: low-pass GNNs, high-pass GNNs, and MLP, via MOE-NP in chameleon.



(b) Ablation study of MOE-NP on the global or local pattern.

Figure 4: Analysis of MOE-NP

	Cora	PubMed	Texas	Cornell	Wisconsin	Chameleon	Actor
Average	79.52 ± 0.81	88.28 ± 0.49	82.70 ± 3.67	82.35 ± 4.64	77.03 ± 5.83	71.29 ± 1.69	36.84 ± 0.87
MOE-NP	89.31 ± 0.91	94.02 ± 0.33	86.76 ± 4.26	86.49 ± 5.54	85.29 ± 3.07	73.82 ± 2.1	40.74 ± 1.36

Table 2: Performance comparison of MOE-NP and using average combination.

Related Work

MOE-NP aims to enhance node classification performance through a mixture of experts framework. The related work is discussed as follows:

Early work introduced the Graph Convolutional Network (GCN) model (Kipf and Welling 2017), which combines spectral filtering of graph signals with non-linearity for supervised node classification. However, GCNs perform suboptimally on heterophilic graphs, which have emerged as a significant challenge in node classification. To address this, specialized models such as GloGNN (Li et al. 2022), LinkX (Lim et al. 2021), LSGNN (Chen et al. 2023), Mixhop (Abu-El-Haija et al. 2019), and ACM-GNN (Luan et al. 2022) have been developed. Recent studies indicate that real-world graphs often exhibit a mix of node patterns (Mao et al. 2024), and traditional GNNs applying the same node patterns across all nodes, can be suboptimal.

The Mixture of Experts (MoE) framework (Jacobs et al. 1991; Jordan and Jacobs 1994) employs a divide-and-conquer strategy to allocate sub-tasks to different experts. It has been widely used in Natural Language Processing (NLP) (Du et al. 2022; Zhou et al. 2022) and Computer Vision (Riquelme et al. 2021). In the graph domain, GraphMETRO (Wu et al. 2023) leverages MoE to address distribution shift issues in GNNs. Link-MoE (Ma et al. 2024) employs multiple GNNs as experts, strategically selecting the most suitable expert for each node pair based on diverse pairwise information.

Conclusion

In this paper, we explored the complex node patterns from different perspectives in the real-world graph datasets and

reveal their influences towards node predictors. To accommodate the diverse needs for node classifiers of different nodes, we propose MOE-NP, a mixture of experts framework for node classification. Specifically, MOE-NP combines a mixture of node predictors and strategically selects models based on node patterns. Extensive experiments demonstrate the proposed MOE-NP demonstrated superior performance on both homophilic and heterophilic datasets. Further, our theoretical analysis and empirical studies validate the rationality and effectiveness of the proposed MOE-NP.

References

- Abu-El-Haija, S.; Perozzi, B.; Kapoor, A.; Alipourfard, N.; Lerman, K.; Harutyunyan, H.; Steeg, G. V.; and Galstyan, A. 2019. MixHop: Higher-Order Graph Convolutional Architectures via Sparsified Neighborhood Mixing. In Chaudhuri, K.; and Salakhutdinov, R., eds., *Proceedings of the 36th International Conference on Machine Learning*, volume 97 of *Proceedings of Machine Learning Research*, 21–29. PMLR.
- Baranwal, A.; Fountoulakis, K.; and Jagannath, A. 2021. Graph Convolution for Semi-Supervised Classification: Improved Linear Separability and Out-of-Distribution Generalization. *ArXiv*, abs/2102.06966.
- Ben Yahia, N. 2024. Enhancing social and collaborative learning using a stacked GNN-based community detection. *Social Network Analysis and Mining*, 14(1): 205.
- Bi, W.; Du, L.; Fu, Q.; Wang, Y.; Han, S.; and Zhang, D. 2024. Make Heterophilic Graphs Better Fit GNN: A Graph Rewiring Approach. *IEEE Transactions on Knowledge and Data Engineering*.

- Chen, Y.; Luo, Y.; Tang, J.; Yang, L.; Qiu, S.; Wang, C.; and Cao, X. 2023. LSGNN: Towards General Graph Neural Network in Node Classification by Local Similarity. In Elkind, E., ed., *Proceedings of the Thirty-Second International Joint Conference on Artificial Intelligence, IJCAI-23*, 3550–3558. International Joint Conferences on Artificial Intelligence Organization.
- Du, N.; Huang, Y.; Dai, A. M.; Tong, S.; Lepikhin, D.; Xu, Y.; Krikun, M.; Zhou, Y.; Yu, A. W.; Firat, O.; et al. 2022. Glam: Efficient scaling of language models with mixture-of-experts. In *International Conference on Machine Learning*, 5547–5569. PMLR.
- Hamilton, W. L.; Ying, R.; and Leskovec, J. 2017. Representation learning on graphs: Methods and applications. *IEEE Data Engineering Bulletin*, 40(3): 52–74.
- Jacobs, R. A.; Jordan, M. I.; Nowlan, S. J.; and Hinton, G. E. 1991. Adaptive mixtures of local experts. *Neural computation*, 3(1): 79–87.
- Jin, W.; Ma, Y.; Wang, Y.; Liu, X.; Tang, J.; Cen, Y.; Qiu, J.; Tang, J.; Shi, C.; Ye, Y.; Zhang, J.; and Yu, P. S. 2021. Graph Representation Learning: Foundations, Methods, Applications and Systems. In *KDD '21: Proceedings of the 27th ACM SIGKDD Conference on Knowledge Discovery & Data Mining*.
- Jordan, M. I.; and Jacobs, R. A. 1994. Hierarchical mixtures of experts and the EM algorithm. *Neural computation*, 6(2): 181–214.
- Kipf, T. N.; and Welling, M. 2017. Semi-supervised classification with graph convolutional networks. *5th International Conference on Learning Representations, ICLR 2017*.
- Li, X.; Zhu, R.; Cheng, Y.; Shan, C.; Luo, S.; Li, D.; and Qian, W. 2022. Finding global homophily in graph neural networks when meeting heterophily. In *International Conference on Machine Learning*, 13242–13256. PMLR.
- Lim, D.; Hohne, F.; Li, X.; Huang, S. L.; Gupta, V.; Bhalerao, O.; and Lim, S. N. 2021. Large scale learning on non-homophilous graphs: New benchmarks and strong simple methods. *Advances in Neural Information Processing Systems*, 34: 20887–20902.
- Lin, G.; Wang, J.; Liao, K.; Zhao, F.; and Chen, W. 2020. Structure fusion based on graph convolutional networks for node classification in citation networks. *Electronics*, 9(3): 432.
- Luan, S.; Hua, C.; Lu, Q.; Zhu, J.; Zhao, M.; Zhang, S.; Chang, X.-W.; and Precup, D. 2022. Revisiting heterophily for graph neural networks. *Advances in neural information processing systems*, 35: 1362–1375.
- Ma, L.; Han, H.; Li, J.; Shomer, H.; Liu, H.; Gao, X.; and Tang, J. 2024. Mixture of Link Predictors. *ArXiv*, abs/2402.08583.
- Ma, Y.; Liu, X.; Shah, N.; and Tang, J. 2021. Is homophily a necessity for graph neural networks? *arXiv preprint arXiv:2106.06134*.
- Mao, H.; Chen, Z.; Jin, W.; Han, H.; Ma, Y.; Zhao, T.; Shah, N.; and Tang, J. 2024. Demystifying structural disparity in graph neural networks: Can one size fit all? *Advances in neural information processing systems*, 36.
- Pei, H.; Wei, B.; Chang, K. C. C.; Lei, Y.; and Yang, B. 2020. GEOM-GCN: GEOMETRIC GRAPH CONVOLUTIONAL NETWORKS. In *8th International Conference on Learning Representations, ICLR 2020*.
- Platonov, O.; Kuznedelev, D.; Babenko, A.; and Prokhorenkova, L. 2024. Characterizing graph datasets for node classification: Homophily-heterophily dichotomy and beyond. *Advances in Neural Information Processing Systems*, 36.
- Riquelme, C.; Puigcerver, J.; Mustafa, B.; Neumann, M.; Jenatton, R.; Susano Pinto, A.; Keyzers, D.; and Houlsby, N. 2021. Scaling vision with sparse mixture of experts. *Advances in Neural Information Processing Systems*, 34: 8583–8595.
- Rozemberczki, B.; Allen, C.; and Sarkar, R. 2021. Multi-scale attributed node embedding. *Journal of Complex Networks*, 9(2): cnab014.
- Sen, P.; Namata, G.; Bilgic, M.; Getoor, L.; Galligher, B.; and Eliassi-Rad, T. 2008. Collective classification in network data. *AI magazine*, 29(3): 93–93.
- Suresh, S.; Budde, V.; Neville, J.; Li, P.; and Ma, J. 2021. Breaking the limit of graph neural networks by improving the assortativity of graphs with local mixing patterns. In *Proceedings of the 27th ACM SIGKDD conference on knowledge discovery & data mining*, 1541–1551.
- Tang, J.; Aggarwal, C.; and Liu, H. 2016. Node classification in signed social networks. In *Proceedings of the 2016 SIAM international conference on data mining*, 54–62. SIAM.
- Wang, J.; Guo, Y.; Yang, L.; and Wang, Y. 2024. Understanding heterophily for graph neural networks. *arXiv preprint arXiv:2401.09125*.
- Wu, S.; Cao, K.; Ribeiro, B.; Zou, J.; and Leskovec, J. 2023. Graphmetro: Mitigating complex distribution shifts in gnns via mixture of aligned experts. *arXiv preprint arXiv:2312.04693*.
- Wu, S.; Sun, F.; Zhang, W.; Xie, X.; and Cui, B. 2022. Graph neural networks in recommender systems: a survey. *ACM Computing Surveys*, 55(5): 1–37.
- Xiao, S.; Wang, S.; Dai, Y.; and Guo, W. 2022. Graph neural networks in node classification: survey and evaluation. *Machine Vision and Applications*, 33(1): 4.
- Yu, B.; Yin, H.; and Zhu, Z. 2018. Spatio-temporal graph convolutional networks: A deep learning framework for traffic forecasting. In *Proceedings of the 27th International Joint Conference on Artificial Intelligence*, 3634–3640. AAAI Press.
- Zheng, Y.; Luan, S.; and Chen, L. 2024. What Is Missing In Homophily? Disentangling Graph Homophily For Graph Neural Networks. *arXiv preprint arXiv:2406.18854*.
- Zhou, Y.; Lei, T.; Liu, H.; Du, N.; Huang, Y.; Zhao, V.; Dai, A. M.; Le, Q. V.; Laudon, J.; et al. 2022. Mixture-of-experts with expert choice routing. *Advances in Neural Information Processing Systems*, 35: 7103–7114.

Appendix

Datasets and Experimental Settings

In this section, we detail the datasets used and the experimental settings for both the baseline models and the proposed MOE-NP framework.

Datasets: We conduct experiments across seven widely recognized datasets, which encompass both homophilic and heterophilic types. These include three homophilic datasets: Cora, Pubmed (Sen et al. 2008); along with three heterophilic datasets: Texas, Wisconsin, Cornell, Chameleon, and Actor (Rozemberczki, Allen, and Sarkar 2021). For all datasets, we generate ten random splits, distributing nodes into 60% training, 20% validation, and 20% testing partitions.

Experimental Settings: For the baseline models, we adopt the same parameter setting in their original paper. For the proposed MOE-NP, we adopt the MLP as the gating model and employ pretrained node predictors as experts. Specifically, we implement the proposed MOE-NP with GCN, GCN with residual connection, High-pass GNN, High-pass GNN with residual connection, and MLP as expert models. We use a single GPU of NVIDIA RTX 4090 24 GB, to run the experiments. All the hyperparameters are tuned based on the validation accuracy from the following search space:

Experts

- Learning Rate: $\{0.0005, 0.001\}$
- Dropout: $\{0 \sim 0.9\}$
- Weight Decay: $\{1e-5, 5e-5, 1e-4\}$
- number of layers = $\{2, 3, 4\}$
- hidden channels = $\{32, 64, 128, 256\}$

MOE-NP

- Gating Learning Rate: $\{0.0005, 0.001\}$
- Gating Weight Decay: $\{1e-5, 5e-5, 1e-4\}$
- Expert Learning Rate: $\{0.001, 0.01, 0.1, 0.5\}$
- Expert Weight Decay: $\{0, 5e-5, 5e-3, 5e-2\}$
- hidden channels = $\{32, 64, 128, 256\}$
- Dropout: $\{0 \sim 0.9\}$
- number of MLP layers : $\{1, 2, 3, 4\}$
- max random walk length : $\{5, 10, 20, 40\}$

Optimization of MOE-NP

There are different optimization strategies for the proposed MOE-NP, such as an end-to-end strategy that training the gating network and the experts simultaneously, or a two-step strategy that training the experts first and then training the gating networks. Some important details are discussed as follows:

(1) load or train?

In a typical mixture of experts (MOE) framework, pretrained expert models are commonly employed for classification tasks, leveraging domain-specific knowledge. For the purpose of capturing distinct node patterns, these pre-trained expert models are more effective at identifying various types

MOE-NP	Cora	Chameleon
w/o few samples	88.45 ± 1.12	71.82 ± 2.2
w few samples	89.31 ± 0.91	73.82 ± 2.1

Table 3: Comparing the performance of models trained with and without using few-samples training experts

of node patterns. If we were to retrain multiple expert models from the ground up, there is a possibility they would capture similar node patterns within the same dataset. Furthermore, considering that the node patterns identified by each expert may differ from those in the dataset, we permit adjustments to the expert model parameters during training, rather than freezing them.

(2) Train experts with fewer samples.

During the training process, we have observed that training the experts on the entire dataset and subsequently training the gating model on the same dataset resulted in a very high initial training accuracy, while the loss decrease was minimal. Consequently, the gating model did not perform as expected. Therefore, we opted to train the experts on a smaller sample, which produced greater loss for the training of the gating model. This approach proved to be more effective than training the experts on the entire dataset. Then we validate the effectiveness of our MOE-NP optimization method by comparing the performance of models trained with and without using few-samples training experts. As shown in Table 3, we present the results for the Cora and Chameleon datasets. It is evident that reducing the sample size of the training experts contributes positively to the overall model performance.

Analysis of the proposed MOE-NP

In this section, we provide more analysis of the proposed MOE-NP. We present the weight distributions of various node predictors in both homophilic and heterophilic datasets, as illustrated in Figures 5, 6, and 7. The results indicate that the gating model can depend on node patterns to allocate different weight combinations.

Analysis the of experts selection

We not only use the model proposed in Empirical Study, also add the two node predictors with residual connection. The node predictor with residual means feeds the information that has never been processed from the original input into the next layer, thereby fully exploiting all the information from the initial node features. Simply aggregating representation from the previous layer might lose important information and consequently incur over-smoothing issues. We use a node predictor with residual that can better obtain more informative intermediate representations and avoid the negative influence of neighbors.

Then we validate the effectiveness of adding the residual experts of node predictors. We compare the performance of models trained with and without the inclusion of residual experts. As shown in Table 4, the results for the Texas and Chameleon datasets are presented. It is evident that adding

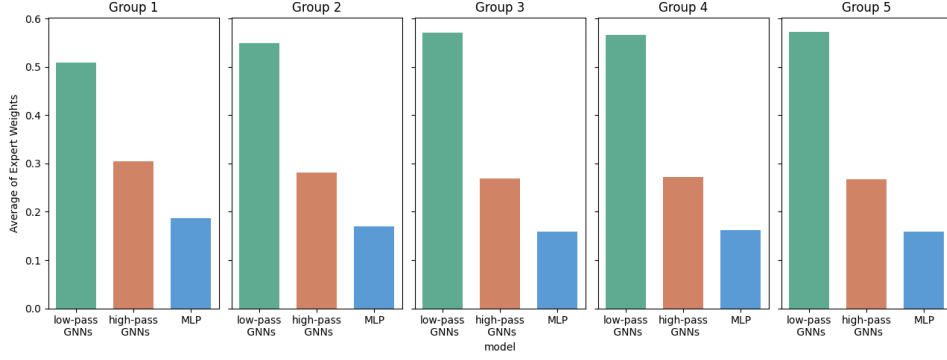


Figure 5: In Cora, the weights assigned to the three experts: low-pass GNNs, high-pass GNNs, and MLP.

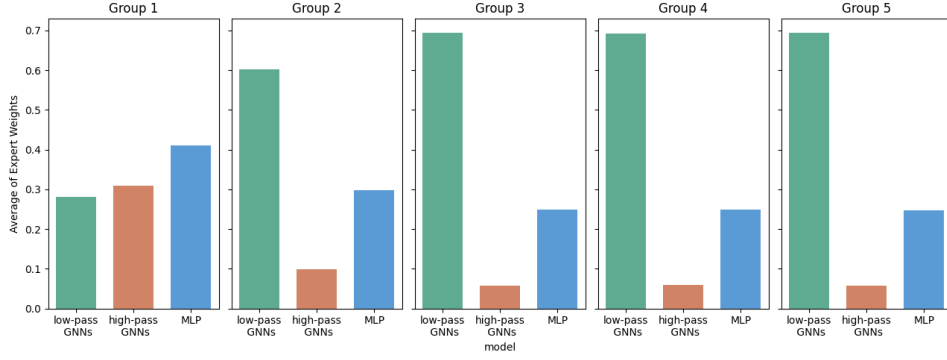


Figure 6: In PubMed, the weights assigned to three experts: low-pass GNNs, high-pass GNNs, and MLP.

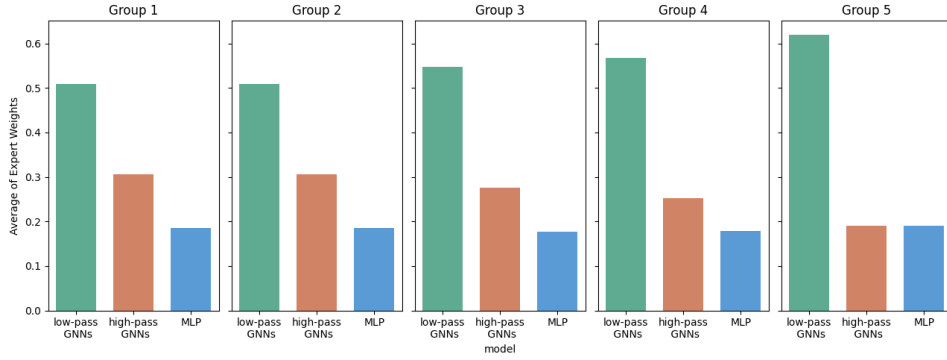


Figure 7: In Actor, the weights assigned to three experts: low-pass GNNs, high-pass GNNs, and MLP.

MOE-NP	texas	Chameleon
w/o residual GNNs	84.9 ± 5.04	73.05 ± 1.44
w residual GNNs	86.76 ± 4.26	73.82 ± 2.1

Table 4: Comparing the performance of models trained with and without using fewer samples training experts

the residual experts of node predictors positively contributes to the overall model performance.

Proofs of Theorem

Proof of Theorem 1 The feature of node i remains normally distributed. Its mean is

$$m(i) = E(\tilde{\mathbf{X}}_i) = \begin{cases} \frac{p\mu + q\nu}{p+q}(1 + o(1)), & \text{for } i \in C_0, \\ \frac{q\mu + p\nu}{p+q}(1 + o(1)), & \text{for } i \in C_1, \end{cases} \quad (9)$$

Here, C_0 and C_1 represent classes 0 and 1. According to Lemma 2 in (Baranwal, Fountoulakis, and Jagannath 2021),

for any unit vector \mathbf{w} , we have

$$\left| \left(\tilde{\mathbf{X}}_i - m(i) \right) \cdot \mathbf{w} \right| = O \left(\sqrt{\frac{\log n}{dn(p+q)}} \right). \quad (10)$$

For $i \in C_0$, we find

$$\begin{aligned} \langle \tilde{\mathbf{X}}_i, \mathbf{w}^* \rangle + b^* &= \frac{\langle p\boldsymbol{\mu} + q\boldsymbol{\nu}, \mathbf{w}^* \rangle}{p+q} (1 + o(1)) + O \left(\|\mathbf{w}^*\| \sqrt{\frac{\log n}{dn(p+q)}} \right) - \frac{1}{2} \langle \boldsymbol{\nu} + \boldsymbol{\mu}, \mathbf{w}^* \rangle \\ &= \frac{\langle 2p\boldsymbol{\mu} + 2q\boldsymbol{\nu} - (p+q)(\boldsymbol{\mu} + \boldsymbol{\nu}), \mathbf{w}^* \rangle}{p+q} (1 + o(1)) + o(\|\mathbf{w}^*\|) \\ &= \frac{p-q}{2(p+q)} \langle \boldsymbol{\mu} - \boldsymbol{\nu}, \mathbf{w}^* \rangle (1 + o(1)) + o(\|\mathbf{w}^*\|) \\ &= -\frac{R(p-q)}{2(p+q)} \|\boldsymbol{\mu} - \boldsymbol{\nu}\| (1 + o(1)) < 0. \end{aligned} \quad (11)$$

Similarly, for $i \in C_1$

$$\langle \tilde{\mathbf{X}}_i, \mathbf{w}^* \rangle + b^* = -\frac{R(q-p)}{2(p+q)} \|\boldsymbol{\mu} - \boldsymbol{\nu}\| (1 + o(1)) > 0. \quad (12)$$

Thus, the classifier with \mathbf{w}^* and b^* successfully separates the classes. However, applying this classifier to $(\mathbf{A}', \mathbf{X}')$ yields

$$\langle \tilde{\mathbf{X}}_i, \mathbf{w}^* \rangle + b^* = \begin{cases} -\frac{R(p'-q')}{2(p'+q')} \|\boldsymbol{\mu} - \boldsymbol{\nu}\| (1 + o(1)) > 0, & \text{for } i \in C_0, \\ -\frac{R(q'-p')}{2(p'+q')} \|\boldsymbol{\mu} - \boldsymbol{\nu}\| (1 + o(1)) < 0, & \text{for } i \in C_1. \end{cases} \quad (13)$$

Consequently, all nodes in $(\mathbf{A}', \mathbf{X}')$ are misclassified. The binary cross-entropy loss over $(\mathbf{A}', \mathbf{X}')$ is

$$L(\mathbf{A}', \mathbf{X}', \mathbf{w}^*, b^*) = \log \left(1 + \exp \left(-\frac{R(p'-q')}{2(p'+q')} \|\boldsymbol{\mu} - \boldsymbol{\nu}\| (1 + o(1)) \right) \right). \quad (14)$$

Since $x = -\frac{R(p'-q')}{2(p'+q')} \|\boldsymbol{\mu} - \boldsymbol{\nu}\| > 0$ implies $e^x \geq x$, it follows that

$$L(\mathbf{A}', \mathbf{X}', \mathbf{w}^*, b^*) \geq \frac{R(q'-p')}{2(p'+q')} \|\boldsymbol{\mu} - \boldsymbol{\nu}\| (1 + o(1)). \quad (15)$$

Proof of Theorem 2 With Eq.(11) and Eq.(12) in the proof of Theorem 1, we can obtain

$$\begin{aligned} L(A', X', \mathbf{w}^*, b^*) &= \frac{1}{n'} \sum_{i=1}^{n'} \log \left(1 + \exp \left((1 - 2\varepsilon_i) (\langle \tilde{\mathbf{X}}'_i, \mathbf{w}^* \rangle + b^*) \right) \right) \\ &\leq \log \left(1 + \exp \left(-\frac{R(p'-q')}{2(p'+q')} \|\boldsymbol{\mu} - \boldsymbol{\nu}\| (1 - o(1)) \right) \right). \end{aligned} \quad (16)$$

Using the inequality $\log(1 + e^{-x}) < Ce^{-x}$, the binary cross-entropy loss can be bounded as

$$L(A', X', \mathbf{w}^*, b^*) \leq C \exp \left(\frac{R(p'-q')}{2(p'+q')} \|\boldsymbol{\mu} - \boldsymbol{\nu}\| (1 - o(1)) \right). \quad (17)$$

This provides an upper bound for the loss, which decays exponentially with the separation parameter.